Chemical Composition of Ultrafine Sea Spray Aerosol during the Sea Spray Chemistry and Particle Evolution (SeaSCAPE) Experiment

*Hayley S. Glicker[1], Michael J. Lawler[1$], Sabrina Chee[1], Julian Resch[2#], Lauren A. Garofalo[3], Kathryn J. Mayer†[4], Kimberly A. Prather[5], Delphine K. Farmer[3], James N. Smith[1]**

[1]Department of Chemistry, The University of California, Irvine, Irvine, CA 92697 USA
[2]Department of Physics, University of Vienna, 1090 Vienna, Austria
[3]Department of Chemistry, Colorado State University, Fort Collins, CO 80523 USA
[4]Department of Chemistry and Biochemistry, University of California, San Diego, La Jolla, CA 92093 USA
[5]Department of Chemistry and Biochemistry and Scripps Institution of Oceanography, University of California, San Diego, La Jolla, CA 92093 USA

*Email: jimsmith@uci.edu

Present Addresses:
[$]M.J.L: Chemical Sciences Laboratory, National Oceanic and Atmospheric Administration, Boulder, CO 80305 USA
[#]J.R.: Department of Environmental Sciences, University of Basel, 4056 Basel, Switzerland.

KEYWORDS: sea spray aerosol, ultrafine, inorganic mass fraction, organic mass fraction, phytoplankton bloom

Abstract

Sea spray is a significant global aerosol source with impacts on marine cloud formation and climate. The physical properties and atmospheric fate of sea spray aerosol depend on its chemical composition, but the current understanding of the sources and composition marine aerosol or sea spray aerosol composition remains limited particularly for the smallest aerosol. The composition of ultrafine (< 100 nm diameter) sea spray aerosol (SSA) particles controls the critical diameter for activation to cloud droplets. This study presents online measurements of sea salt and organic mass fractions in ultrafine sea spray aerosol measured during the Sea Spray Chemistry and Particle Evolution (SeaSCAPE) experiment conducted in summer 2019 at Scripps Institution of Oceanography. Primary sea spray aerosol particles were generated in a wave flume mesocosm study with coastal seawater obtained from Scripps Pier in San Diego, CA. Ultrafine particle composition measurements were performed using the Thermal Desorption Chemical Ionization Mass Spectrometer (TDCIMS). Trends in inorganic and organic fractions show dependence on the biological activity of the ocean water, where heterotrophic bacteria concentrations were correlated with organic mass fraction of ultrafine sea spray aerosol. At low phytoplankton concentrations, ultrafine sea spray particles were mainly composed of inorganic salts. Characteristic positive ion fragments indicate influence from polysaccharides and fatty acids likely of bacterial origin in the smallest sizes. In contrast, polysaccharide and fatty acid species were below detection levels in TDCIMS measurements of larger sea spray aerosol (~100-200 nm). Comparisons with submicron aerosol composition measured by an Aerosol Mass Spectrometer (AMS) showed high correlation between AMS and general TDCIMS organic fractions but anti-correlation between measured, individual TDCIMS organics. These results

suggest biological drivers for inorganic and organic aerosol composition and a strong size dependence on the organic composition of nascent sea spray, consistent with previous findings.

1. Introduction

Atmospheric aerosol plays a critical role in the Earth's radiative budget but remain the single largest source of uncertainty in models estimating potential changes in radiative forcing.[1,2] The atmospheric impacts of particles are dependent upon multiple factors including composition, size, and number concentration, which can all affect their ability to serve as cloud condensation nuclei (CCN).[3–5] Sea spray aerosol (SSA) are an important contributor to total aerosol mass globally.[6,7] SSA can activate into cloud droplets, which have been shown to potentially change the albedo of marine boundary layer clouds by as much as 30%.[8] The composition of SSA, especially the sea salt component, impacts the ability to serve as cloud droplets, due to the hygroscopicity of these chemical components.[9] It is important to understand the processes that control SSA production and composition because of the significant role of it plays in Earth's radiative budget.[10]

Sea spray aerosol (SSA) is produced via physical ejection of sea spray droplets produced by bubble-bursting.[7,11–13] Two major mechanisms for SSA formation occur during bubble bursting. Submicron particles are mainly produced through the rupture of film droplets, which contain surface-active molecules such as aliphatic organics that are enriched in the sea surface microlayer relative to bulk seawater.[14–16] Supermicron particles are understood to be formed via jet droplets that often closely reflect the composition of bulk seawater, composed of sea salt with dissolved organic species and potentially large fragments from organisms. Submicron SSA composition, especially in the sub-100 nm size range, is of particular

68 importance as the chemical composition within this size range directly affects the particles'
69 ability to form a cloud droplet and nucleate as a CCN.[6]

70 Both field and laboratory studies have been performed in an effort to determine the
71 composition of ultrafine SSA, but each pose unique challenges. Prior work has established
72 that freshly emitted SSA undergoes rapid chemical changes under ambient conditions due to
73 the uptake of acidic gases, water loss, and other aging processes, with results from field
74 measurements suggesting a change in pH could take place over timescales ranging from
75 minutes to hours.[17,18] Field measurements represent a non-controlled environment, where
76 measurements of SSA composition are often limited to remote regions with little
77 anthropogenic influence.[7] Even within this location restriction, sampling of freshly emitted,
78 SSA is extremely difficult and essentially no ambient measurements can provide information
79 on nascent SSA. There is a substantial amount of previous work that supports the view that
80 SSA contains marine biogenic organics.[19–22] As a result, there is still uncertainty as to the
81 extent of the influence that marine biological activity has on SSA organic composition and
82 the size-dependence of particle composition.[13,21,22] Additionally, commonly utilized
83 laboratory techniques to produce SSA do not appropriately mimic the production of SSA,
84 and thus the particle physicochemical properties are not representative of those in the real
85 world.[23]

86 This study focuses on online measurements of ultrafine nascent sea spray aerosol using
87 the Thermal Desorption Chemical Ionization Mass Spectrometer (TDCIMS) and reports
88 trends in the inorganic and organic composition during the Sea Spray and Particle Evolution
89 experiment (SeaSCAPE).[24] Utilizing the wave channel located in the Hydraulics Laboratory
90 at Scripps Institution of Oceanography, this experiment simulated the coastal marine air-sea

interface in a laboratory setting by inducing phytoplankton blooms in collected seawater to mimic marine biological activity and inducing regular wave-breaking SSA formation. This study investigates the trends in inorganic and organic composition of ultrafine sea spray aerosol and potential connections to biological activity. Additionally, TDCIMS measurements of the integrated, sub-200 nm nascent aerosol and complementary composition measurements of submicron non-refractory aerosol from an Aerosol Mass Spectrometer (AMS) allow further insights into the size-resolved composition of submicron SSA.

2. Methods

a. SeaSCAPE campaign and sampling configuration

The Sea Spray Chemistry and Particle Evolution (SeaSCAPE) experiment was conducted at the Scripps Institution of Oceanography in the summer of 2019. This experiment utilized a sealed, 11,800 L wave channel filled with coastal Pacific Ocean seawater to mimic the ocean-atmosphere interface. A mechanical paddle generated waves that broke at an artificial beach to simulate wave breaking aerosol formation mechanisms and produce realistic SSA. This experiment was conducted over two months and was divided into three phytoplankton blooms, each induced by the addition of growth media to promote phytoplankton growth. Further descriptions of the experiment specifications and schematics, the bloom initiation process, nutrient information and measurements performed can be found in Sauer et al., 2022. The work presented herein characterizes ultrafine SSA from the second bloom, which took place from July 13 to July 20, 2019. The second bloom, unlike the later bloom, utilized a 50-μm Nitex mesh filter directly on the pump while filling the wave flume with seawater which unintentionally damaged some of the microorganisms present in the seawater. However, this does not necessarily make

the seawater less representative of the real marine environment, as lysing of phytoplankton cells may take place naturally due to predation by bacteria and viruses. Nutrients were added two days after the initial fill of the tank with algae growth media and sodium metasilicate to promote phytoplankton growth. Taxonomy classification during the field experiment is discussed in more detail in Sauer et al., 2022. Ultrafine SSA measurements presented herein were measured via sampling ports located roughly 3 m downstream of the artificial beach.

b. Thermal Desorption Chemical Ionization Mass Spectrometry (TDCIMS)

Ultrafine SSA particle composition was measured using TDCIMS. This instrument has been described in detail in prior manuscripts.[25–27] The TDCIMS sampled air from the wave channel headspace slightly behind the artificial beach where wave breaking occurred . Sample air passed through unipolar chargers (UPCs) to charge ultrafine SSA via ion diffusion.[28] Negatively charged particles were then size-selected in radial differential mobility analyzers (RDMAs). Two UPC/RDMA units operated in parallel. Charged, size-selected particles were then electrostatically deposited onto a Pt wire for a designated amount of time. For this experiment, ultrafine SSA were collected for one hour to achieve sufficient particle mass collected while maintaining good temporal resolution. Once the collection was complete, the wire was translated into the ion source region where thermal desorption was performed. The wire was resistively heated over a programmed temperature ramp from about room temperature to a sufficiently high temperature to volatilize aerosol NaCl (estimated 800℃) over a period of 70 s. Chemical components of the sampled SSA were desorbed according to their volatilities.

Following desorption, reagent ions reacted with desorbed compounds to form product ions, which were detected with a time-of-flight mass spectrometer. The reagent ions for negative ion mode were O_2^- and $(H_2O)_nO_2^-$ clusters, and for positive ion mode reagent ions were H_3O^+ and

larger protonated water clusters. Only one polarity could be observed for a given aerosol sample. Sampling of SSA during the SeaSCAPE experiment was set for one hour, followed by a one-hour background, then switching polarities. Background measurements followed the same sampling procedures as the collections, but without applying a voltage to the Pt wire. Background signals primarily resulted from gases adsorbed onto the wire and to the walls of the ion source. For the current study we integrated collection and background ion signals over the entire desorption period, with exception of the Na^+ ion described below. Signals reported herein are background-subtracted signals that are normalized at every point by the average reagent ion signal to account for changing sensitivity of the instrument as the campaign progressed. Signal and concentration uncertainties are based on the ion counting variability, calculated as the square root of the ion count.

c. Quantification of NaCl mass fractions and organic ion mass fractions

i. Quantification of Inorganic Mass Fractions

Quantification of NaCl mass fraction in SSA was performed using overnight data for each of the 8 days of the second bloom. Overnight particle populations were relatively stable in comparison to daytime, enabling accurate estimations of collected particulate mass. We hypothesize this variability during the day due to changing temperature and flume conditions. Collected mass was calculated using measurements of number-size distributions from a scanning mobility particle sizer (SMPS), which consisted of a bipolar neutralizer, nano DMA (model 3085; TSI Inc.) and mixing condensation particle sizer (MCPC, model 1720, Brechtel). A separate, identical MCPC operated in parallel to provide integrated particle number concentration. Both instruments sampled the exit flow of the TDCIMS inlet, downstream of the collection filament. For these measurements, the TDCIMS RDMAs were set to 300 V,

corresponding to a mobility diameter of 25 nm. The physical size distribution of collected particles depends on the size distribution of particles in the wave channel headspace, since particles larger than 20 nm in diameter are subject to multiple-charging by the UPC.[29] This physical size distribution was captured by the downstream SMPS equipped with a bipolar neutralizer.

To estimate sampled particulate mass, we first determined the campaign-averaged, size-resolved collection efficiency for the range of particle diameters delivered to the TDCIMS (Figure S1). The uncertainties in collection efficiency and collected particle mass were atypically high for these measurements due to the low particle concentrations, particularly at the target sizes. This collection efficiency was then applied to the average size distribution during a background sampling period to determine the average size distribution of particles collected during the adjacent sampling period, which we used to determine the volume mean diameter of sampled particles. Average volume concentration of sampled particles was determined by multiplying the volume mean diameter by $\overline{N}_{coll} - \overline{N}_{back}$, where $\overline{N}_{coll}$ and $\overline{N}_{back}$ are the average number concentration of particles measured by the separate MCPC during the adjacent collection and background periods, respectively. Multiplying the average volume concentration by the sample flow rate and collection time, and assuming a density of sodium chloride (2.16 g/cm^3), we estimated sampled particulate mass.

Inorganic particulate mass was quantified based on the TDCIMS-derived sodium ion signal. Na^+ was the primary ion utilized for quantification purposes, due to the potential influence from chloride-containing gaseous species or sample volatilization effects on the Cl^- integrated signal. Sodium chloride atomized particles were collected to determine the relationship between measured ion abundance and sample mass. The broad, multiply peaked Na^+

183 thermogram of collected SSA suggests multiple processes may be responsible for the formation
184 of Na^+ ions during desorption (Figure S2). We attribute the first peak in the thermogram to
185 inorganic Na^+ from melting NaCl which volatilized after melting, due to its correlation to both
186 the $ClNa_2^+$ ion, which can only be derived from NaCl, and the peak Na^+ signal of atomized NaCl
187 particles. We used this peak for quantification. To confirm the validity of this approach, we also
188 compared thermograms of laboratory atomized NaCl to a sea salt standard (Sigma Aldrich).
189 Signal integration of the whole thermogram yielded a non-linear relationship between ion
190 abundance and collected particulate mass (Figure S3). However, the integration of only the mode
191 associated with the first major desorption peak around 37 s results in an ion abundance-to-
192 collected mass relationship that is linear and comparable for both NaCl and sea salt atomized
193 standards. We therefore use this first peak to determine the contribution of NaCl to particulate
194 mass. Later desorption peaks, after 40 seconds, may be due to direct emission of Na^+ ions from
195 the wire via thermal emission. Prior work has shown the potential for the thermal emission of
196 sodium and potassium ions when corresponding alkali halides were heated on platinum to similar
197 temperatures found in the TDCIMS.[30]

198 To integrate the first peak in the Na^+ thermogram, the entire thermogram was modeled as
199 the sum of five Gaussian distributions using a numerical optimization package (Igor Pro function
200 optimize m=3, simulated annealing). This process always resulted in a separate Gaussian mode
201 with a peak at 37 s, as shown in Figure S2. The mass of sampled particulate NaCl in the SSA
202 was then calculated using calibration data from the first Gaussian mode of the Na^+ signal from
203 NaCl atomized standards (Figure S4). This mass of particulate NaCl was divided by the total
204 sampled SSA particulate mass measured during the same sampling period to obtain the time
205 series of inorganic mass fractions.

ii. Quantification of Organic Ion Components in Ultrafine SSA

It was not possible to quantify the majority of organic components present in the ultrafine SSA. Due to the multitude of species present in the organic portion of the composition, total mass quantification based on standards is unrealistic. As a result, we report the abundance of characteristic ions normalized by collected particulate mass. Prior TDCIMS measurements of ambient marine aerosol have identified, via positive matrix factorization (PMF), characteristic polysaccharide and fatty acid factors.[19] These strongest and most characteristic fragments from PMF analysis of polysaccharide species, $C_5H_5O_2^+$ and $C_6H_5O_3^+$, and of fatty acid species, $C_{14}H_{29}O_2^+$, were identified during the SeaSCAPE campaign and used for relative quantification. Nanocellulose is a useful calibration species for polysaccharides in the TDCIMS[19], and we used it as a standard in this study as well. Assuming these characteristic polysaccharide fragments are primarily from polysaccharides in the SSA samples, the mass of polysaccharide-like material in SSA can be estimated (Figure S5).

While polysaccharide and fatty acid components may comprise a significant portion of organic nascent aerosol, it is important to note that there are other organic species present in sea spray aerosol that the TDCIMS is less sensitive to. For example, the TDCIMS has poor sensitivity to humic-like substances, which have been previously found to contribute to primary marine organic aerosol.[19,31–33] One likely reason for this is the complex, irregular structure of such substances, which result in a broad distribution of ions in the TDCIMS. Other complex biogenic molecules may be similarly difficult to detect. Organic analysis herein focuses on TDCIMS-sensitive organic components.

iii. Quantification of Sub-200 nm SSA Organic Ion Fractions

In order to compare the composition of ultrafine SSA and larger submicron (100-200 nm) particles, measurements of the latter were made every morning during bloom 2. The sampling approach is the same to that of the TDCIMS ultrafine particle collection approach noted above, but the RDMA voltage was increased to 1100 V and the sampling time was shortened to 1 min. While this voltage corresponds to a 50 nm mobility diameter, multiple charging and a size distribution centered at greater than 100 nm resulted in particles of 100-200 nm dominating the sample mass. Since the TDCIMS downstream SMPS could not measure the full range of particle sizes collected, a different approach was taken to determine particulate mass collected as required for the calculation of ion fractions. Assuming that the majority of particulate mass collected at larger particle sizes is inorganic sea salt, which is dominated by NaCl and quantifiable by the Na^+ ion, we calculate sample mass based on the abundance of this ion using the same method described above.

d. Complementary aerosol and biological seawater measurements

The chemical composition of submicron non-refractory aerosol was measured by high resolution time-of-flight aerosol mass spectrometry (HR-TOF-AMS; Aerodyne Research Inc.).[34] Dry nascent SSA size distributions (d_m = 13.8 – 723.4 nm) were measured from the wave channel headspace using an SMPS equipped with an X-ray neutralizer (TSI Inc, Classifier 3080, DMA 3081, WCPC 3787). Details of the SMPS and AMS operation during SeaSCAPE are described elsewhere.[24]Measurements of the taxonomic composition of bulk seawater utilized whole seawater sampling with viable cell enumeration using confocal microscopy and i*n vivo* chlorophyll *a* concentrations were continuously measured via an Environmental Sample Processor during the experiment.[24] Bulk seawater samples collected daily utilized 16S and 18S rDNA amplicon sequencing to measure the microbial and chemical composition as the bloom

progressed.[35] This sequencing allows for the understanding of the progression of various bacterial classes.

e. Principal component analysis

Principal component analysis (PCA) was performed with the "princomp" function of the R statistical software package (R,2011) similar to the approach explained in Glicker et al. (2019). This analysis included key polysaccharide and fatty acid TDCIMS positive ion signal fractions, as well as TDCIMS-measured NaCl Fraction, AMS chloride and organic fractions, total heterotrophic cell concentration and sub-700 nm integrated particle number from size distribution measurements.

3. Results and Discussion

a. Inorganic Mass Fraction

During the second bloom, the average integrated number concentration of sub-100 nm diameter particles during overnight collections was 99 ± 22 particles/cm^3. The TDCIMS sampled SSA with a volume mean diameter of ~40 nm (Figure 1). Given the low particle concentrations, sample masses were typically within the range of 150-400 pg after one-hour collections (Fig. S4). SSA particle size distributions associated with the early bloom, prior to July 16th, 2019, show generally lower number concentrations of sub-100 nm particles, but have a similar characteristic distribution compared to later bloom size distributions. We considered the possibility that background contamination particles could affect the calculated mass measurements. In comparing the average nightly distributions during the early and late periods of the blooms, the late bloom aerosol concentration is enhanced, on average, a factor of 1.7 ± 0.2 for every size bin, making this amplification of particle number uniform throughout all particle

diameters measured (Figure S6). From this we conclude that there is not likely any bias caused by background particles, and that concentration changes result from processes occurring in the wave flume.

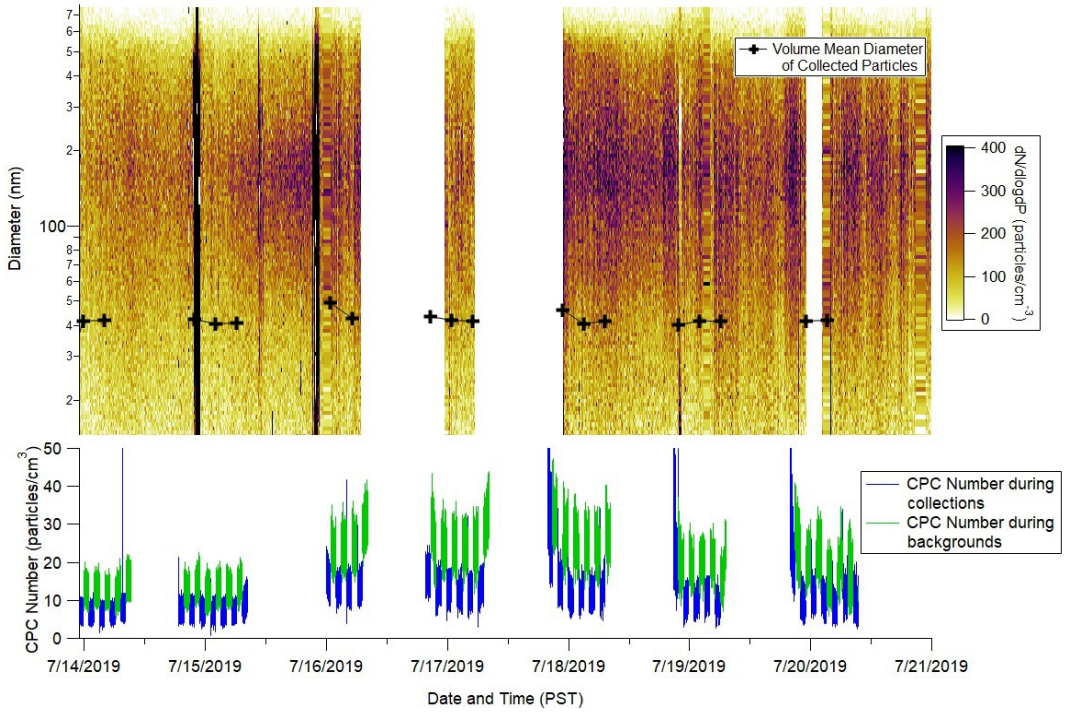

Figure 1: The particle size distribution of nascent sea spray aerosol during bloom 2 of the SeaSCAPE campaign. The volume mean diameter of particles collected (black crosses) is approximately 40 nm. As noted in the methods section c.i., the difference between background CPC and collection CPC counts, on the bottom plot, with the volume mean diameter were used to estimate mass of collected particles. Background CPC counts are associated with particle counts when there is no voltage applied to the TDCIMS Pt wire, whereas collection CPC counts are associated to the particle counts when a voltage is applied.

To obtain the inorganic mass fraction, the calculated NaCl mass was divided at each overnight collection by the total sample mass of particles as described above. The trend in time series of the inorganic fraction is shown in Figure 2. The inorganic fraction reported is the fraction of only NaCl, as any other seawater salts are expected to contribute only a small fraction to the mass compared with the uncertainty of these measurements.[37] The main source of

uncertainty in mass fraction is due to the uncertainties associated with the size-resolved collection efficiency of the TDCIMS (Figure S1). Especially at small mass loadings like those measured in this study, the particulate mass estimated is sensitive to slight changes in collected average volume mean diameter, with the largest size-dependent collection efficiency uncertainty of +/- 20% for 40 nm sampled particles. Early bloom 2 has relatively low inorganic fractions and, as the bloom progresses, the inorganic mass fraction increases. Samples with low inorganic mass are assumed to have correspondingly high organic fractions, as we are unable to quantify organic mass directly using calibrations.

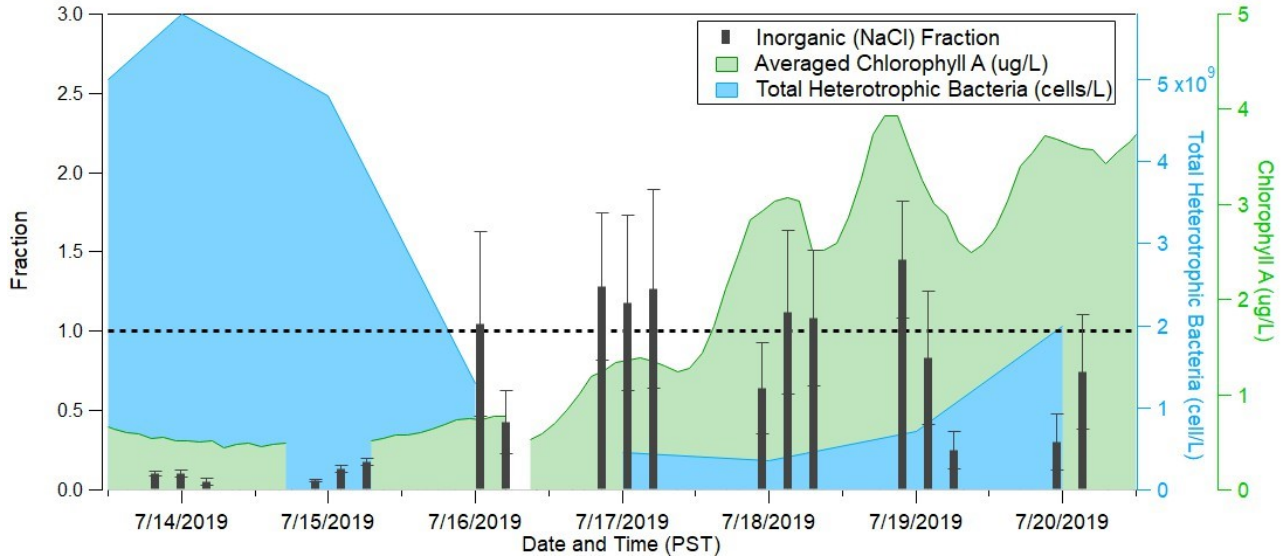

Figure 2: Inorganic mass fraction (vertical, dark gray bars) measured from sodium chloride during bloom 2. The black dashed line denotes a fraction of 1. Shaded blue regions are measured total heterotrophic cell concentration in cells/L and shaded green regions are measured chlorophyll *a* concentration in ug/L.

Organic fraction was highest during the first two days of the bloom (Figure 2). This coincides with peak biological activity as determined by total concentration of viable cells. At the start of this bloom, over-filtered water was utilized which led to the lysing of cells, eventually leading to a decrease in cell concentration three days into the bloom. Neither bulk seawater nor

295 the sea surface microlayer was otherwise affected by this filtration. As the living cells died by
296 July 16th, inorganic fraction began to peak. The higher biological activity earlier may have
297 corresponded with higher seawater concentrations of organics that preferentially contributed to
298 SSA. These similar results of the relationship between biological activity and organic fraction
299 have been previously observed in O'Dowd et al. (2004) and Prather et al. (2013).

300 b. Organic fraction of sub-100 nm nascent sea spray particles

301 Insights into organic composition can be obtained from the variety of ions detected by
302 TDCIMS. From prior TDCIMS measurements of marine aerosol, various fragments were
303 identified belonging to a few key organic sources.[19] In this prior work, Lawler et al. used positive
304 matrix factorization (PMF) to identify five characteristic organic types in filter-sampled marine
305 aerosol collected over the North Atlantic. These factors correspond to polysaccharides,
306 recalcitrant organics, fatty acids, and two types of oxidized secondary organics. For the present
307 measurements of nascent sea spray aerosol, where secondary chemistry was assumed to be
308 negligible, the dominant and most characteristic peaks of the polysaccharide and fatty acid
309 factors were expected to be most abundant in these SeaSCAPE measurements.

310 Biogenic polysaccharides have been found to contribute to the composition of marine
311 aerosol, where marine phytoplankton produce polysaccharides that contribute to the organic
312 carbon pool.[19,39] Figure 3 shows plots of mass-normalized ion abundance of two polysaccharides
313 and one fatty acid ions that were major ions in the corresponding PMF factors. No attempt was
314 made to calibrate for fatty acids or recalcitrant organic compounds; however, by normalizing by
315 sample mass we are able to investigate relative changes in these species during the course of the
316 campaign. As stated previously, polysaccharidal material was characterized by the positive ion
317 fragments $C_5H_5O_2^+$ and $C_6H_5O_3^+$. Polysaccharide mass estimates were quantified using

laboratory standards and peak mass from these species was roughly 200 pg (Figure S5). Polysaccharide mass fractions for ultrafine sea spray aerosol were quantified and suggest contributions ranging for <1% to as much as 60% of the total mass, as shown in Figure S5. These estimates are upper bounds since other chemical species could result in these ion fragments. Polysaccharides have been previously measured in laboratory sea spray aerosol samples and in ambient marine aerosol and suggest a similar wide range of impact on particle composition.[19,40,41] The link between the enrichment of polysaccharides in sea spray aerosol and marine bacteria has been observed[42] and is explored further in section D of the results.

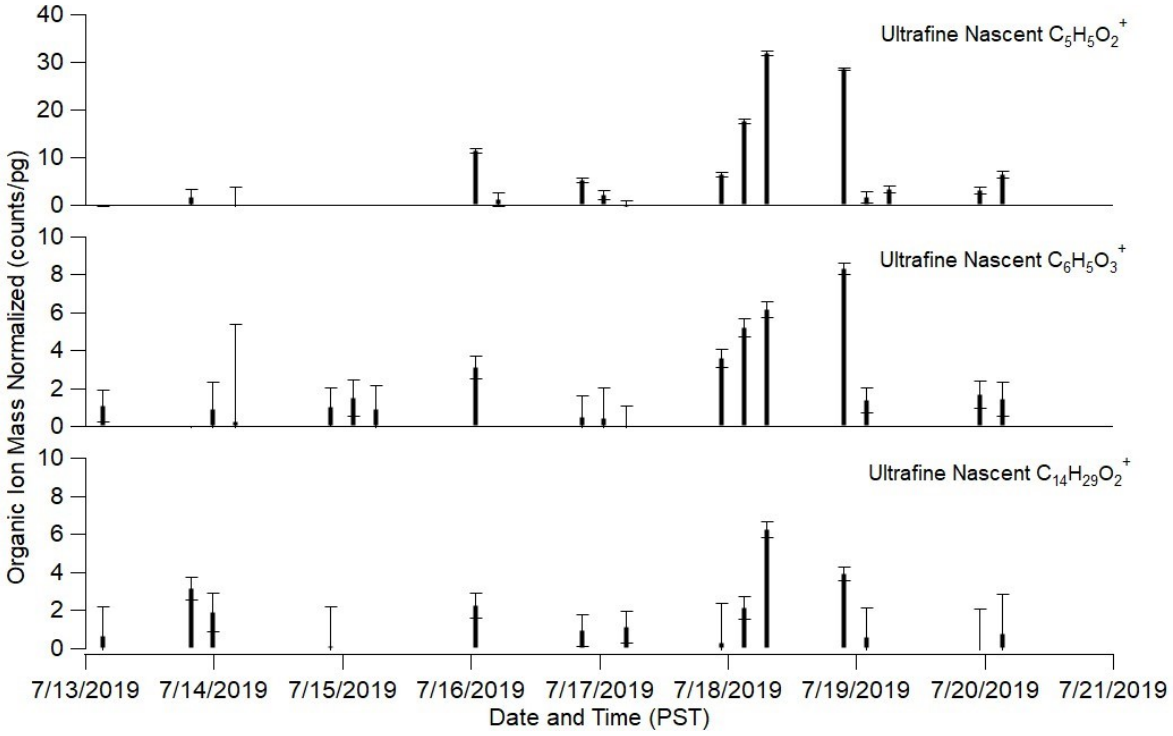

Figure 3: Time series of the organic ion abundance of $C_5H_5O_2^+$, $C_6H_5O_3^+$ and $C_{14}H_{29}O_2^+$ mass normalized by the total mass of particles collected. $C_5H_5O_2^+$ and $C_6H_5O_3^+$ are identified as polysaccharide tracers and $C_{14}H_{29}O_2^+$ is a fatty acid. Error bars are propagated from uncertainties in TDCIMS ion abundance and sample mass measurements.

The ion $C_{14}H_{29}O_2^+$ is linked to fatty acid contribution, namely from myristic acid and other aliphatic fragments. Other, smaller, hydrocarbon fragments were additionally measured during the second bloom. Fatty acids have been previously measured in marine aerosol, largely attributed to lipase enzymatic activity of lipid constituents and other marine biota.[19,43–46] The peak in fatty acid contribution mirrored that of polysaccharidal species. Trends in these species over bloom 2 were similar to those of the inorganic mass fraction, peaking towards the second half of the bloom. While these species were present throughout the whole campaign, the peak in mass-normalized ion abundance was unexpected as the organic fraction of ultrafine nascent sea spray aerosol peaked within the first two days. This indicates that, when the inorganic contribution to sub-100 nm sea spray aerosol was largest, the polysaccharides and fatty acids were at their highest levels. The explanation of this observed trend could be linked to the generally lower total sub-100 nm particulate mass collected for the first two days of the campaign (Figure S4). With lower total particulate mass collected, the masses of these individual polysaccharide or fatty acid species may be smaller, even with a more dominant organic fraction. Even though a smaller mass of particles was collected early in the measurement time, since a larger fraction of those particles were organic in nature, these polysaccharide or fatty acid species would be measured if they were readily available. It is important to reiterate that, during the times of peak organic ultrafine SSA fraction, the mass-normalized abundance of the corresponding ions above were low. During the first half of the bloom, the TDCIMS-detected organics were relatively low, signifying that the dominant organics in ultrafine SSA were organics that the TDCIMS is not sensitive to. These species present during the highest organic fraction time may be humic-like substances or other complex biogenic molecules, as these species lead to a broad distribution of ions in the TDCIMS. However, the observed trend of these polysaccharide and fatty acid species

could also be influenced by the organic enrichment, as noted in the chlorophyll *a* concentrations, during the second half of bloom.

c. Organic fraction 100-200 nm diameter nascent sea spray particles

In an effort to gain insight into size-dependent particle composition, the organic constituents of TDCIMS-analyzed 100-200 nm aerosol can be compared to the ultrafine composition detailed above. Early morning 100-200 nm measurements during bloom 2 had significantly larger total mass collected, as estimated using collected NaCl mass. The average collected NaCl mass during the 1-minute collections was 1300 ± 260 pg. Given this approach for estimating sample mass, this would likely underestimate total particulate mass, but still suggests a drastic increase to the total collected mass when compared to 1 hour collections of sub-60 nm particles.

Figure 4 shows the mass-normalized time series of the three most important identified organic components for both the sub-100 nm and 100-200 nm diameter particles. Across all these fragments, there were significantly smaller organic mass-normalized ion abundances for these larger particles and no real peaks in the mass spectra for these species, even given the larger, underestimated total mass of 100-200 nm collected particle samples that would likely over-predict mass-normalized ion abundance,. This suggests a significant size-dependence in the particle composition for these compounds detected by the TDCIMS. Previous work has generally noted that along with a decrease in diameter there is an increase in the organic composition of sea spray aerosol.[47] However, TDCIMS measurements of the same organic ion fragments for these two different particle size populations show that there is a size-resolved impact on the organic composition and types of organics present. Fatty acid species and polysaccharide species

are significantly lower in the integrated sub-200 nm aerosol population compared to sub-100 nm particles.

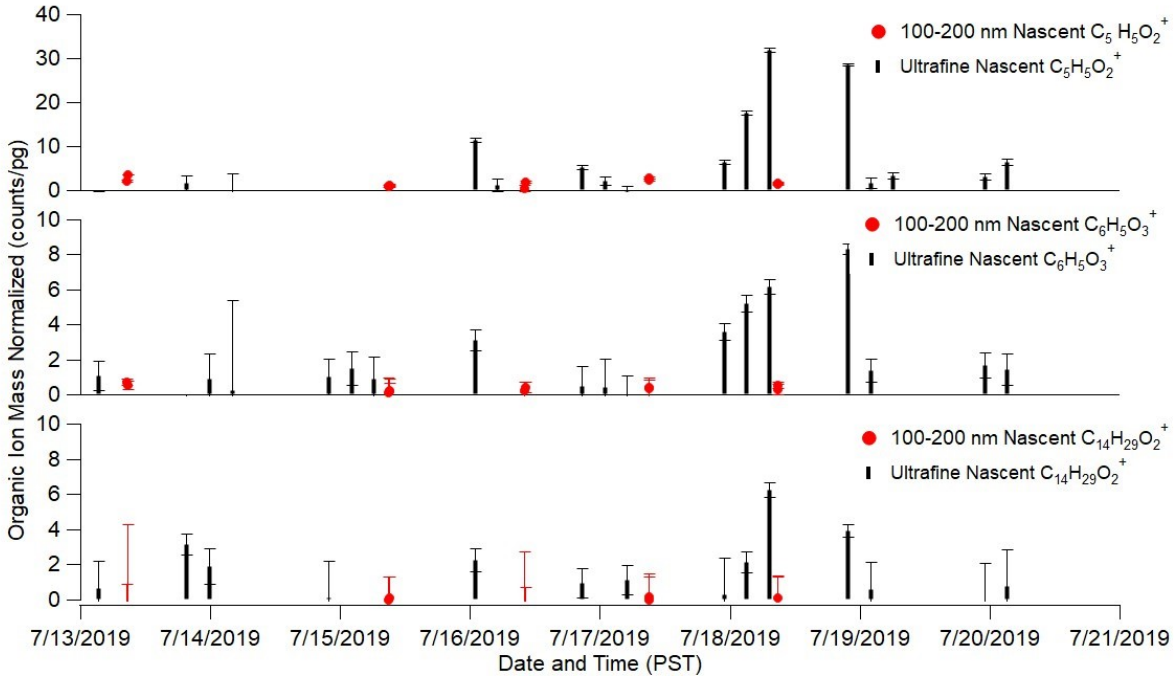

Figure 4: Sub-100 nm (black) and 100-200 nm (red) diameter mass-normalized organic ion signals for three characteristic primary organic fragments, $C_5H_5O_2^+$, $C_6H_5O_3^+$ and $C_{14}H_{29}O_2^+$. While fatty acid and polysaccharide species were a significant component of TDCIMS measured species in sub-100 nm particles, these organic fragments were significantly lower in the integrated sub-200 nm aerosol population.

To evaluate potential sources and contributions to both the inorganic and organic fractions, TDCIMS-measured inorganic and organic fractions were compared to AMS-derived mass fractions via Principal Component Analysis (PCA). Figure 5 shows the results of this analysis. Tightly correlated species, like TDCIMS NaCl fraction and AMS Chloride fraction, are represented by a large aspect ratio of the displayed ellipse. Such correlations may denote similar sources, as these two fractions from each measurement are from inorganic salts present in SSA. Additionally, the strong correlation between TDCIMS and AMS inorganic fractions and sub-700 nm integrated number indicates there is a strong

relationship between the inorganic salt contribution and presence of sea spray aerosol across TDCIMS and AMS aerosol size populations. However, the AMS organic fraction is anti-correlated with most TDCIMS-sensitive organic species individually but correlated with the overall organic fraction of sub-100 nm particles as determined by the subtraction of the measured inorganic fraction as described above. The correlation between the TDCIMS and AMS organic fractions suggest that broader influences of organics may impact different particle size populations similarly, like the general trend in biological activity, but the anti-correlation between individual TDCIMS organics suggests that the organic composition is chemically different between these groups. This idea is reinforced by the direct comparisons of TDCIMS-measured organics in sub-100 nm and 100-200 nm samples. The TDCIMS measurements of 100-200 nm diameter particles would likely be associated with the smallest sizes measured by the AMS, so AMS mass fractions analyzed here would be largely represented by larger TDCIMS-analyzed particles. In the comparison of these three size populations, sub-100 nm particles seem to have a unique organic chemical composition, comprised of polysaccharides and fatty acids. This is not observed in sea spray aerosol particles greater than 100 nm in diameter.

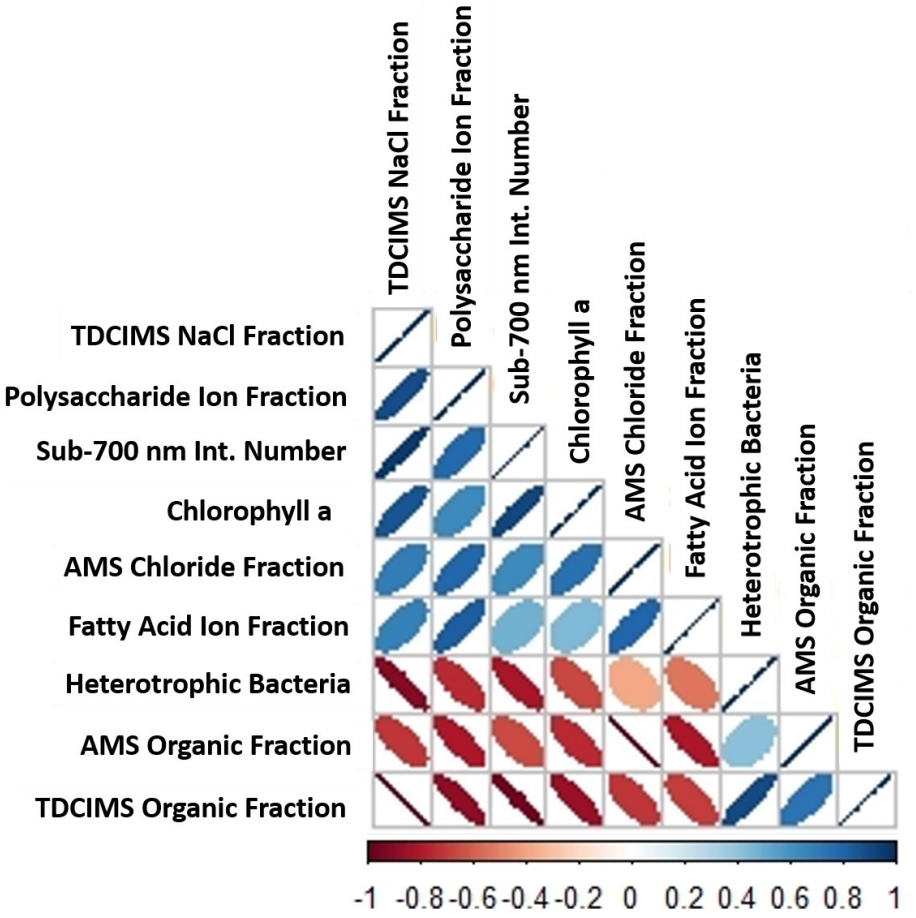

Figure 5: Principal component analysis (PCA) of TDCIMS organic and inorganic fractions, AMS organic and inorganic fraction, heterotrophic cell concentration in ug/L and sub 700 nm integrated particles number data. Polysaccharide Ion Fraction is the average ion fraction of $C_5H_5O_2^+$ and $C_6H_5O_3^+$ for ultrafine nascent particles and Fatty Acid Ion fraction is the average ion fraction of $C_{14}H_{29}O_2^+$ in ultrafine nascent particles. Species shown are ordered with decreasing correlation to the first principal component, from the top to the bottom. The darker blue, narrower positive slope ellipse notes stronger correlation and the darker red, narrower negative slope ellipse notes stronger anti-correlation.

400

401 d. Potential biological influence and implications

402 The potential relationship between sea spray aerosol and seawater biology has been evaluated
403 in numerous studies.[14,38,48] TDCIMS-measured organics in sub-100 nm sea spray aerosol may be
404 linked to the presence of various classes of bacteria present during the bloom progression. The

405 presence of bacteria connected to polysaccharide-producing and degrading enzymes, noted in
406 Figure S5, showed a similar trend in relative abundance.[46,49] Marine bacteria have been shown to
407 have an effect on saccharide enrichment in sea spray aerosol.[42,50] Certain strains of heterotrophic
408 bacteria, like those investigated in Figure S5, directly impact the composition and size of
409 saccharides present in seawater, thus impacting the sea spray aerosol composition.[42,50] These
410 bacteria thrive in the presence of various algal-polysaccharides that are typically found in marine
411 environments and are critical in the degradation of intact cell-wall polysaccharides. Therefore, as
412 the bloom progressed, leading to the increase in abundance of these polysaccharide-related
413 bacteria, this may have led to an increase in the mass-normalized organic ion signal for these two
414 polysaccharide species. The fatty acid component of organic composition may be linked to
415 lipase-producing bacteria. While the lipase activity leading to the production of free fatty acids
416 can vary depending on the bacterial species and organic medium, previous work has investigated
417 the lipid degradation rate for marine lipase-producing bacteria in a triglyceride-enriched medium
418 to simulate marine environments. [51] Results of that work showed that free fatty acids began to
419 appear via lipase enzymatic reactions from tripalmitate after 19 hours. As free fatty acids are
420 produced via lipase activity over the timescale of several hours, it seems that the sub-100 nm
421 particulate composition may be influenced in a similar manner. While initial attempts to directly
422 connect the ultrafine nascent aerosol composition to biological activity can only be achieved
423 with this work, additional work in the future can help elucidate the complex connection between
424 particle composition and marine biological activity.

425 **4. Conclusions**

426 The inorganic mass fraction and some organic components of ultrafine sea spray aerosol
427 were measured during the 2019 SeaSCAPE experiment at the Scripps Institution of

Oceanography. The inorganic component dominated the mass fraction of ultrafine particles at times of low phytoplankton activity. During times of higher biological activity as determined by the total sea water cell count, the organic fraction dominated, but inorganic sodium chloride was still present. The TDCIMS was not very sensitive to the organic components present during high organic mass fraction periods, indicating that these organics could be humic-like substances or other complex organic compounds that are not sensitively detected by TDCIMS. Clear fatty acid and polysaccharide signals were only measured in the ultrafine size range, despite greater sample mass for 100-200 nm particles. These measurements are the first to compare these two SSA particle size populations using the TDCIMS technique, and showed that the organic composition of ultrafine particles differs greatly from only modestly larger particles, despite both being film drop-generated. Similar trends in both organic and inorganic fractions were observed for both TDCIMS- and AMS-measured SSA, but TDCIMS results suggest that different organic species influence the composition of the two particle populations. As the composition directly impacts particle physicochemical properties and ultimately atmospheric fate, more work is needed to understand the composition of ultrafine SSA produced during times of both high and low biological activity. The fate of inorganic ultrafine particles would inherently be different than organic ultrafine particles, thus leading to different aging processes and CCN formation.

Associated Content

Supporting Information

Collection efficiency of ultrafine particles via TDCIMS measurements (Figure S1), Gaussian parameterized desorption analysis for sodium chloride (Figure S2), non-linear vs linear fits for Na+ signal using Gaussian parametrization (Figure S3), estimated total mass of particles collected and estimated mass of sodium chloride (Figure S4), estimated mass of polysaccharide

species and polysaccharide mass fractions (Figure S5), size distributions at different parts of the campaign measurements to rule out background influence (Figure S6)

Author Information

Corresponding Author

James N. Smith- *Department of Chemistry, The University of California, Irvine, Irvine, CA 92697, United States;* orcid.org/0000-0003-4677-8224; Email: jimsmith@uci.edu

Authors

Hayley S. Glicker- *Department of Chemistry, The University of California, Irvine, Irvine, CA 92697, United States*

Michael J. Lawler- *Department of Chemistry, The University of California, Irvine, Irvine, CA 92697, United States*

Sabrina Chee- *Department of Chemistry, The University of California, Irvine, Irvine, CA 92697, United States*

Julian Resch- *Department of Physics, University of Vienna, Vienna, Austria*

Lauren A. Garofalo- *Department of Chemistry, Colorado State University, Fort Collins, CO 80523, United States*

Kathryn J. Mayer- *Department of Chemistry and Biochemistry, University of California, San Diego, La Jolla, CA 92093, United States.* Current: *Department of Chemistry, Colorado State University, Fort Collins, CO 80523, United States*

Kimberly A. Prather - *Department of Chemistry and Biochemistry and Scripps Institution of*

Oceanography, University of California, San Diego, La Jolla, CA 92093, United States

Delphine K. Farmer- *Department of Chemistry, Colorado State University, Fort Collins, CO 80523, United States*

James N. Smith- *Department of Chemistry, The University of California, Irvine, Irvine, CA 92697, United States*

Notes

The authors declare no competing financial interest

Acknowledgments

This work was supported by the US National Science Foundation (AGS-1762098). All authors would like to thank the NSF Center for Aerosol Impacts on Chemistry of the Environment (CAICE), an NSF-Funded Center for Chemical Innovation (CHE-1801971). In particular, the authors acknowledge the contributions of Chris Cappa, Tim Bertram, Chris Lee and Jon Sauer for their planning and organization of SeaSCAPE. KJM and KAP would like to thank Cristina Bahaveolos, Catherine Mullenmeister and Chi Min Ni who assisted with the SMPS data collection.

References

(1) Stocker, T. F.; Qin, D.; Plattner, G.-K.; Tignor, M. S. K.; Allen, J.; Boschung, A.; Nauels, Y.; Xia, X.; Midgley, P. M. *IPCC Climate Change 2013: The Physical Science Basis. Contribution of Working Group I to the Fifth Assessment Report of the Intergovernmental Panel on Climate Change*; 2013.

(2) Bellouin, N.; Quaas, J.; Gryspeerdt, E.; Kinne, S.; Stier, P.; Watson-Parris, D.; Boucher,

O.; Carslaw, K. S.; Christensen, M.; Daniau, A. L.; Dufresne, J. L.; Feingold, G.; Fiedler, S.; Forster, P.; Gettelman, A.; Haywood, J. M.; Lohmann, U.; Malavelle, F.; Mauritsen, T.; McCoy, D. T.; Myhre, G.; Mülmenstädt, J.; Neubauer, D.; Possner, A.; Rugenstein, M.; Sato, Y.; Schulz, M.; Schwartz, S. E.; Sourdeval, O.; Storelvmo, T.; Toll, V.; Winker, D.; Stevens, B. Bounding Global Aerosol Radiative Forcing of Climate Change. *Reviews of Geophysics*. Blackwell Publishing Ltd March 1, 2020. https://doi.org/10.1029/2019RG000660.

(3) Broekhuizen, K.; Chang, R. Y. W.; Leaitch, W. R.; Li, S. M.; Abbatt, J. P. D. Closure between Measured and Modeled Cloud Condensation Nuclei (CCN) Using Size-Resolved Aerosol Compositions in Downtown Toronto. *Atmospheric Chemistry and Physics*. 2006, pp 2513–2524. https://doi.org/10.5194/acp-6-2513-2006.

(4) Lohmann, U.; Feichter, J. Global Indirect Aerosol Effects: A Review. *Atmospheric Chemistry and Physics*. European Geosciences Union 2005, pp 715–737. https://doi.org/10.5194/acp-5-715-2005.

(5) Pöschl, U. Atmospheric Aerosols: Composition, Transformation, Climate and Health Effects. *Angewandte Chemie - International Edition*. John Wiley & Sons, Ltd November 25, 2005, pp 7520–7540. https://doi.org/10.1002/anie.200501122.

(6) Gantt, B.; Meskhidze, N. The Physical and Chemical Characteristics of Marine Primary Organic Aerosol: A Review. *Atmospheric Chemistry and Physics*. 2013, pp 3979–3996. https://doi.org/10.5194/acp-13-3979-2013.

(7) O'Dowd, C. D.; De Leeuw, G. Marine Aerosol Production: A Review of the Current Knowledge. *Philosophical Transactions of the Royal Society A: Mathematical, Physical*

514 *and Engineering Sciences*. 2007, pp 1753–1774. https://doi.org/10.1098/rsta.2007.2043.

515 (8) Fossum, K. N.; Ovadnevaite, J.; Ceburnis, D.; Preißler, J.; Snider, J. R.; Huang, R. J.;
516 Zuend, A.; O'Dowd, C. Sea-Spray Regulates Sulfate Cloud Droplet Activation over
517 Oceans. *npj Clim. Atmos. Sci.* **2020**, *3* (1). https://doi.org/10.1038/s41612-020-0116-2.

518 (9) Rosati, B.; Christiansen, S.; Dinesen, A.; Roldin, P.; Massling, A.; Nilsson, E. D.; Bilde,
519 M. The Impact of Atmospheric Oxidation on Hygroscopicity and Cloud Droplet
520 Activation of Inorganic Sea Spray Aerosol. *Sci. Rep.* **2021**, *11* (1), 10008.
521 https://doi.org/10.1038/s41598-021-89346-6.

522 (10) Rap, A.; Scott, C. E.; Spracklen, D. V; Bellouin, N.; Forster, P. M.; Carslaw, K. S.;
523 Schmidt, A.; Mann, G. Natural Aerosol Direct and Indirect Radiative Effects. *Geophys.*
524 *Res. Lett.* **2013**, *40* (12), 3297–3301. https://doi.org/10.1002/grl.50441.

525 (11) Stokes, M. D.; Deane, G. B.; Prather, K.; Bertram, T. H.; Ruppel, M. J.; Ryder, O. S.;
526 Brady, J. M.; Zhao, D. A Marine Aerosol Reference Tank System as a Breaking Wave
527 Analogue for the Production of Foam and Sea-Spray Aerosols. *Atmos. Meas. Tech.* **2013**,
528 *6* (4), 1085–1094. https://doi.org/10.5194/amt-6-1085-2013.

529 (12) Deane, G. B.; Stokes, M. D. Scale Dependence of Bubble Creation Mechanisms in
530 Breaking Waves. *Nature* **2002**, *418* (6900), 839–844. https://doi.org/10.1038/nature00967.

531 (13) Cochran, R. E.; Ryder, O. S.; Grassian, V. H.; Prather, K. A. Sea Spray Aerosol: The
532 Chemical Link between the Oceans, Atmosphere, and Climate. *Accounts of Chemical*
533 *Research*. 2017, pp 599–604. https://doi.org/10.1021/acs.accounts.6b00603.

534 (14) Wang, X.; Sultana, C. M.; Trueblood, J.; Hill, T. C. J.; Malfatti, F.; Lee, C.; Laskina, O.;

Moore, K. A.; Beall, C. M.; McCluskey, C. S.; Cornwell, G. C.; Zhou, Y.; Cox, J. L.; Pendergraft, M. A.; Santander, M. V.; Bertram, T. H.; Cappa, C. D.; Azam, F.; DeMott, P. J.; Grassian, V. H.; Prather, K. A. Microbial Control of Sea Spray Aerosol Composition: A Tale of Two Blooms. *ACS Cent. Sci.* **2015**, *1* (3), 124–131. https://doi.org/10.1021/acscentsci.5b00148.

(15) Lewis, E. R.; Schwartz, S. E. Sea Salt Aerosol Production: Mechanisms, Methods, Measurements and Models—A Critical Review. In *Geophysical Monograph Series*; Geophysical Monograph Series; American Geophysical Union: Washington, D. C., 2004; Vol. 152, pp 1–408. https://doi.org/10.1029/152GM01.

(16) Wang, X.; Deane, G. B.; Moore, K. A.; Ryder, O. S.; Stokes, M. D.; Beall, C. M.; Collins, D. B.; Santander, M. V.; Burrows, S. M.; Sultana, C. M.; Prather, K. A. The Role of Jet and Film Drops in Controlling the Mixing State of Submicron Sea Spray Aerosol Particles. *Proc. Natl. Acad. Sci. U. S. A.* **2017**, *114* (27), 6978–6983. https://doi.org/10.1073/pnas.1702420114.

(17) Angle, K. J.; Crocker, D. R.; Simpson, R. M. C.; Mayer, K. J.; Garofalo, L. A.; Moore, A. N.; Mora Garcia, S. L.; Or, V. W.; Srinivasan, S.; Farhan, M.; Sauer, J. S.; Lee, C.; Pothier, M. A.; Farmer, D. K.; Martz, T. R.; Bertram, T. H.; Cappa, C. D.; Prather, K. A.; Grassian, V. H. Acidity across the Interface from the Ocean Surface to Sea Spray Aerosol. *Proc. Natl. Acad. Sci. U. S. A.* **2021**, *118* (2). https://doi.org/10.1073/pnas.2018397118.

(18) Fridlind, A. M.; Jacobson, M. Z. A Study of Gas-Aerosol Equilibrium and Aerosol PH in the Remote Marine Boundary Layer during the First Aerosol Characterization Experiment (ACE 1). *J. Geophys. Res. Atmos.* **2000**, *105* (D13), 17325–17340.

https://doi.org/10.1029/2000JD900209.

(19) Lawler, M. J.; Lewis, S. L.; Russell, L. M.; Quinn, P. K.; Bates, T. S.; Coffman, D. J.; Upchurch, L. M.; Saltzman, E. S. North Atlantic Marine Organic Aerosol Characterized by Novel Offline Thermal Desorption Mass Spectrometry: Polysaccharides, Recalcitrant Material, and Secondary Organics. *Atmos. Chem. Phys.* **2020**, *20* (24), 16007–16022. https://doi.org/10.5194/acp-20-16007-2020.

(20) Parungo, F. P.; Nagamoto, C. T.; Rosinski, J.; Haagenson, P. L. A Study of Marine Aerosols over the Pacific Ocean. *J. Atmos. Chem.* **1986**, *4* (2), 199–226. https://doi.org/10.1007/BF00052001.

(21) Bigg, E. K.; Leck, C. The Composition of Fragments of Bubbles Bursting at the Ocean Surface. *J. Geophys. Res. Atmos.* **2008**, *113* (11). https://doi.org/10.1029/2007JD009078.

(22) O'Dowd, C. D.; Facchini, M. C.; Cavalli, F.; Ceburnis, D.; Mircea, M.; Decesari, S.; Fuzzi, S.; Young, J. Y.; Putaud, J. P. Biogenically Driven Organic Contribution to Marine Aerosol. *Nature* **2004**, *431* (7009), 676–680. https://doi.org/10.1038/nature02959.

(23) Collins, D. B.; Zhao, D. F.; Ruppel, M. J.; Laskina, O.; Grandquist, J. R.; Modini, R. L.; Stokes, M. D.; Russell, L. M.; Bertram, T. H.; Grassian, V. H.; Deane, G. B.; Prather, K. A. Direct Aerosol Chemical Composition Measurements to Evaluate the Physicochemical Differences between Controlled Sea Spray Aerosol Generation Schemes. *Atmos. Meas. Tech.* **2014**, *7* (11), 3667–3683. https://doi.org/10.5194/amt-7-3667-2014.

(24) Sauer, J. S.; Mayer, K. J.; Lee, C.; Alves, M. R.; Amiri, S.; Bahaveolos, C. J.; Franklin, E. B.; Crocker, D. R.; Dang, D.; Dinasquet, J.; Garofalo, L. A.; Kaluarachchi, C. P.; Kilgour, D. B.; Mael, L. E.; Mitts, B. A.; Moon, D. R.; Moore, A. N.; Morris, C. K.;

Mullenmeister, C. A.; Ni, C.-M.; Pendergraft, M. A.; Petras, D.; Simpson, R. M. C.; Smith, S.; Tumminello, P. R.; Walker, J. L.; DeMott, P. J.; Farmer, D. K.; Goldstein, A. H.; Grassian, V. H.; Jaffe, J. S.; Malfatti, F.; Martz, T. R.; Slade, J. H.; Tivanski, A. V; Bertram, T. H.; Cappa, C. D.; Prather, K. A. The Sea Spray Chemistry and Particle Evolution Study (SeaSCAPE): Overview and Experimental Methods. *Environ. Sci. Process. Impacts* **2022**, *24* (2), 290–315. https://doi.org/10.1039/d1em00260k.

(25) Smith, J. N.; Moore, K. F.; McMurry, P. H.; Eisele, F. L. Atmospheric Measurements of Sub-20 Nm Diameter Particle Chemical Composition by Thermal Desorption Chemical Ionization Mass Spectrometry. *Aerosol Sci. Technol.* **2004**, *38* (2), 100–110. https://doi.org/10.1080/02786820490249036.

(26) Voisin, D.; Smith, J. N.; Sakurai, H.; Mcmurry, P. H.; Eisele, F. L. Thermal Desorption Chemical Ionization Mass Spectrometer for Ultrafine Particle Chemical Composition. *Aerosol Sci. Technol.* **2003**, *37* (37), 471–475. https://doi.org/10.1080/02786820390125232.

(27) Lawler, M. J.; Whitehead, J.; C.O'Dowd; C.Monahan; McFiggans, G.; Smith, J. N. Composition of 15–85 Nm Particles in Marine Air. *Atmos. Chem. Phys.* **2014**, *14*, 11557–11569.

(28) Chen, D. R.; Pui, D. Y. H. A High Efficiency, High Throughput Unipolar Aerosol Charger for Nanoparticles. *J. Nanoparticle Res.* **1999**, *1* (1), 115–126. https://doi.org/10.1023/A:1010087311616.

(29) Mcmurry, P. H.; Ghimire, A.; Ahn, H. K.; Sakurai, H.; Moore, K.; Stolzenburg, M.; Smith, J. N. Sampling Nanoparticles for Chemical Analysis by Low Resolution Electrical

Mobility Classification. *Environ. Sci. Technol.* **2009**, *43* (13), 4653–4658. https://doi.org/10.1021/es8029335.

(30) Toubes, B.; Rollefson, G. K. The Nature of the Ions Emitted by Heated Filaments and Salts. *J. Chem. Phys.* **1940**, *8* (6), 495–496. https://doi.org/10.1063/1.1750693.

(31) Rinaldi, M.; Decesari, S.; Finessi, E.; Giulianelli, L.; Carbone, C.; Fuzzi, S.; O'Dowd, C. D.; Ceburnis, D.; Facchini, M. C. Primary and Secondary Organic Marine Aerosol and Oceanic Biological Activity: Recent Results and New Perspectives for Future Studies. *Adv. Meteorol.* **2010**, *2010*, 1–10. https://doi.org/10.1155/2010/310682.

(32) Santander, M. V.; Mitts, B. A.; Pendergraft, M. A.; Dinasquet, J.; Lee, C.; Moore, A. N.; Cancelada, L. B.; Kimble, K. A.; Malfatti, F.; Prather, K. A. Tandem Fluorescence Measurements of Organic Matter and Bacteria Released in Sea Spray Aerosols. *Environ. Sci. Technol.* **2021**, *55* (8), 5171–5179. https://doi.org/10.1021/acs.est.0c05493.

(33) Santander, M. V.; Schiffer, J. M.; Lee, C.; Axson, J. L.; Tauber, M. J.; Prather, K. A. Factors Controlling the Transfer of Biogenic Organic Species from Seawater to Sea Spray Aerosol. *Sci. Rep.* **2022**, *12* (1), 1–11. https://doi.org/10.1038/s41598-022-07335-9.

(34) DeCarlo, P. F.; Kimmel, J. R.; Trimborn, A.; Northway, M. J.; Jayne, J. T.; Aiken, A. C.; Gonin, M.; Fuhrer, K.; Horvath, T.; Docherty, K. S.; Worsnop, D. R.; Jimenez, J. L. Field-Deployable, High-Resolution, Time-of-Flight Aerosol Mass Spectrometer. *Anal. Chem.* **2006**, *78* (24), 8281–8289. https://doi.org/10.1021/ac061249n.

(35) Aron, A. T.; Gentry, E. C.; McPhail, K. L.; Nothias, L. F.; Nothias-Esposito, M.; Bouslimani, A.; Petras, D.; Gauglitz, J. M.; Sikora, N.; Vargas, F.; van der Hooft, J. J. J.; Ernst, M.; Kang, K. Bin; Aceves, C. M.; Caraballo-Rodríguez, A. M.; Koester, I.; Weldon,

K. C.; Bertrand, S.; Roullier, C.; Sun, K.; Tehan, R. M.; Boya P, C. A.; Christian, M. H.; Gutiérrez, M.; Ulloa, A. M.; Tejeda Mora, J. A.; Mojica-Flores, R.; Lakey-Beitia, J.; Vásquez-Chaves, V.; Zhang, Y.; Calderón, A. I.; Tayler, N.; Keyzers, R. A.; Tugizimana, F.; Ndlovu, N.; Aksenov, A. A.; Jarmusch, A. K.; Schmid, R.; Truman, A. W.; Bandeira, N.; Wang, M.; Dorrestein, P. C. Reproducible Molecular Networking of Untargeted Mass Spectrometry Data Using GNPS. *Nat. Protoc.* **2020**, *15* (6), 1954–1991. https://doi.org/10.1038/s41596-020-0317-5.

(36) Glicker, H. S.; Lawler, M. J.; Ortega, J.; De Sá, S. S.; Martin, S. T.; Artaxo, P.; Vega Bustillos, O.; De Souza, R.; Tota, J.; Carlton, A.; Smith, J. N. Chemical Composition of Ultrafine Aerosol Particles in Central Amazonia during the Wet Season. *Atmos. Chem. Phys.* **2019**, *19* (20), 13053–13066. https://doi.org/10.5194/acp-19-13053-2019.

(37) Lyman, J.; Fleming, R. H. Composition of Sea Water. *J. Mar. Res.* **1940**, *3*, 134–146.

(38) Prather, K. A.; Bertram, T. H.; Grassian, V. H.; Deane, G. B.; Stokes, M. D.; DeMott, P. J.; Aluwihare, L. I.; Palenik, B. P.; Azam, F.; Seinfeld, J. H.; Moffet, R. C.; Molina, M. J.; Cappa, C. D.; Geiger, F. M.; Roberts, G. C.; Russell, L. M.; Ault, A. P.; Baltrusaitis, J.; Collins, D. B.; Corrigan, C. E.; Cuadra-Rodriguez, L. A.; Ebben, C. J.; Forestieri, S. D.; Guasco, T. L.; Hersey, S. P.; Kim, M. J.; Lambert, W. F.; Modini, R. L.; Mui, W.; Pedler, B. E.; Ruppel, M. J.; Ryder, O. S.; Schoepp, N. G.; Sullivan, R. C.; Zhao, D. Bringing the Ocean into the Laboratory to Probe the Chemical Complexity of Sea Spray Aerosol. *Proc. Natl. Acad. Sci. U. S. A.* **2013**, *110* (19), 7550–7555. https://doi.org/10.1073/pnas.1300262110.

(39) Orellana, M. V.; Leck, C. Marine Microgels. In *Biogeochemistry of Marine Dissolved*

Organic Matter: Second Edition; Elsevier Inc., 2015; pp 451–480. https://doi.org/10.1016/B978-0-12-405940-5.00009-1.

(40) Aller, J. Y.; Radway, J. A. C.; Kilthau, W. P.; Bothe, D. W.; Wilson, T. W.; Vaillancourt, R. D.; Quinn, P. K.; Coffman, D. J.; Murray, B. J.; Knopf, D. A. Size-Resolved Characterization of the Polysaccharidic and Proteinaceous Components of Sea Spray Aerosol. *Atmos. Environ.* **2017**, *154*, 331–347. https://doi.org/10.1016/j.atmosenv.2017.01.053.

(41) Cochran, R. E.; Laskina, O.; Trueblood, J. V.; Estillore, A. D.; Morris, H. S.; Jayarathne, T.; Sultana, C. M.; Lee, C.; Lin, P.; Laskin, J.; Laskin, A.; Dowling, J. A.; Qin, Z.; Cappa, C. D.; Bertram, T. H.; Tivanski, A. V.; Stone, E. A.; Prather, K. A.; Grassian, V. H. Molecular Diversity of Sea Spray Aerosol Particles: Impact of Ocean Biology on Particle Composition and Hygroscopicity. *Chem* **2017**, *2* (5), 655–667. https://doi.org/10.1016/j.chempr.2017.03.007.

(42) Hasenecz, E. S.; Jayarathne, T.; Pendergraft, M. A.; Santander, M. V; Mayer, K. J.; Sauer, J.; Lee, C.; Gibson, W. S.; Kruse, S. M.; Malfatti, F.; Prather, K. A.; Stone, E. A. Marine Bacteria Affect Saccharide Enrichment in Sea Spray Aerosol during a Phytoplankton Bloom. *ACS Earth Sp. Chem.* **2020**, *4* (9), 1638–1649. https://doi.org/10.1021/acsearthspacechem.0c00167.

(43) Tervahattu, H.; Juhanoja, J.; Kupiainen, K. Identification of an Organic Coating on Marine Aerosol Particles by TOF-SIMS. *J. Geophys. Res. Atmos.* **2002**, *107* (16), ACH 18-1. https://doi.org/10.1029/2001JD001403.

(44) Bikkina, P.; Kawamura, K.; Bikkina, S.; Kunwar, B.; Tanaka, K.; Suzuki, K. Hydroxy

667 Fatty Acids in Remote Marine Aerosols over the Pacific Ocean: Impact of Biological
668 Activity and Wind Speed. *ACS Earth Sp. Chem.* **2019**, *3* (3), 366–379.
669 https://doi.org/10.1021/acsearthspacechem.8b00161.

670 (45) Mochida, M.; Kitamori, Y.; Kawamura, K.; Nojiri, Y.; Suzuki, K. Fatty Acids in the
671 Marine Atmosphere: Factors Governing Their Concentrations and Evaluation of Organic
672 Films on Sea-Salt Particles. *J. Geophys. Res. Atmos.* **2002**, *107* (17), AAC 1-1-AAC 1-10.
673 https://doi.org/10.1029/2001JD001278.

674 (46) Zhang, C.; Kim, S. K. Research and Application of Marine Microbial Enzymes: Status
675 and Prospects. *Marine Drugs*. MDPI AG 2010, pp 1920–1934.
676 https://doi.org/10.3390/md8061920.

677 (47) Ault, A. P.; Moffet, R. C.; Baltrusaitis, J.; Collins, D. B.; Ruppel, M. J.; Cuadra-
678 Rodriguez, L. A.; Zhao, D.; Guasco, T. L.; Ebben, C. J.; Geiger, F. M.; Bertram, T. H.;
679 Prather, K. A.; Grassian, V. H. Size-Dependent Changes in Sea Spray Aerosol
680 Composition and Properties with Different Seawater Conditions. *Environ. Sci. Technol.*
681 **2013**, *47* (11), 5603–5612. https://doi.org/10.1021/es400416g.

682 (48) Freney, E.; Sellegri, K.; Nicosia, A.; Williams, L. R.; Rinaldi, M.; Trueblood, J. T.;
683 Prévôt, A. S. H.; Thyssen, M.; Grégori, G.; Haëntjens, N.; DInasquet, J.; Obernosterer, I.;
684 Van Wambeke, F.; Engel, A.; Zäncker, B.; Desboeufs, K.; Asmi, E.; Timonen, H.; Guieu,
685 C. Mediterranean Nascent Sea Spray Organic Aerosol and Relationships with Seawater
686 Biogeochemistry. *Atmos. Chem. Phys.* **2021**, *21* (13), 10625–10641.
687 https://doi.org/10.5194/acp-21-10625-2021.

688 (49) Martin, M.; Barbeyron, T.; Martin, R.; Portetelle, D.; Michel, G.; Vandenbol, M. The

Cultivable Surface Microbiota of the Brown Alga Ascophyllum Nodosum Is Enriched in Macroalgal-Polysaccharide-Degrading Bacteria. *Front. Microbiol.* **2015**, *6* (DEC), 1487. https://doi.org/10.3389/fmicb.2015.01487.

(50) Hasenecz, E. S.; Kaluarachchi, C. P.; Lee, H. D.; Tivanski, A. V; Stone, E. A. Saccharide Transfer to Sea Spray Aerosol Enhanced by Surface Activity, Calcium, and Protein Interactions. *ACS Earth Sp. Chem.* **2019**, *3* (11), 2539–2548. https://doi.org/10.1021/acsearthspacechem.9b00197.

(51) Duflos, M.; Goutx, M.; Van Wambeke, F. Determination of Lipid Degradation by Marine Lipase-Producing Bacteria: Critical Evaluation of Lipase Activity Assays. *Lipids* **2009**, *44* (12), 1113–1124. https://doi.org/10.1007/s11745-009-3358-7.

701 **For TOC Only**

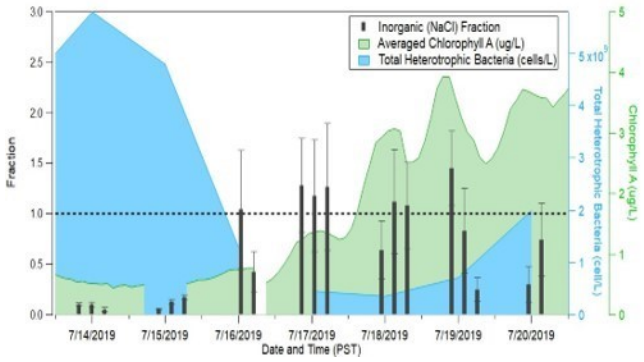

702